Phase plates for generation of variable amounts of primary spherical aberration

Eva Acosta[1,*] and José Sasián[2]

[1]*Area de Óptica, Departamento de Física Aplicada, Facultad de Física, Universidad de Santiago de Compostela, 15782, Spain*

[2]*The University of Arizona, College of Optical Sciences, Meinel Building, 1630 E. University Blvd., Tucson, AZ 85721, USA*

**eva.acosta@usc.es*

Abstract: We discuss a set of phase plate-pairs for the generation of variable amounts of primary spherical aberration. The surface descriptions of these optical plates are provided, and their aberration-generating properties are verified with real ray-tracing. These plate-pairs are robust in that they allow large tolerances to spacing as well as errors in the relative displacement of the plates. Both primary spherical aberration (r^4) and Zernike spherical aberration ($6r^4 - 6r^2 + 1$) can be generated. The amount of spherical aberration is proportional to the plate-pair displacement and in our example it reaches up to 48 waves (~8 waves Zernike) for a clear aperture of 25 mm.

OCIS codes: (220.0220) Optical design and fabrication; (220.1000) Aberration compensation.

References and links

1. P. S. Tsai, B. Migliori, K. Campbell, T. N. Kim, Z. Kam, A. Groisman, and D. Kleinfeld, "Spherical aberration correction in nonlinear microscopy and optical ablation using a transparent deformable membrane," Appl. Phys. Lett. **91**(19), 191102 (2007).
2. E. Theofanidou, L. Wilson, W. Hossack, and J. Arlt, "Spherical aberration correction for optical tweezers," Opt. Commun. **236**(1-3), 145–150 (2004).
3. J. Knittel, H. Richter, M. Hain, S. Somalingam, and T. Tschudi, "Liquid crystal lens for spherical aberration compensation in blu-ray disc systems," IEE Proc. Sci. Meas. Technol. **152**(1), 15–18 (2005).
4. P. Mouroulis, "Depth of field extension with spherical optics," Opt. Express **16**(17), 12995–13004 (2008).
5. M. Schwertner, M. J. Booth, T. Tanaka, T. Wilson, and S. Kawata, "Spherical aberration correction system using an adaptive optics deformable mirror," Opt. Commun. **263**(2), 147–151 (2006).
6. R. A. Buchroeder and R. B. Hooker, "Aberration generator," Appl. Opt. **14**(10), 2476–2479 (1975).
7. L. W. Alvarez and W. E. Humphrey, "Variable power lens and system," U.S. Patent 3,507,565 (1970).
8. L. W. Alvarez, "Two-element variable-power spherical lens," U.S. Patent 3,305,294 (1967).
9. A. W. Lohmann, "A new class of varifocal lenses," Appl. Opt. **9**(7), 1669–1671 (1970).
10. S. Bará, Z. Jaroszewicz, A. Kołodziejczyk, and V. Moreno, "Determination of basic grids for subtractive moire patterns," Appl. Opt. **30**(10), 1258–1262 (1991).
11. A. W. Lohmann and D. P. Paris, "Variable Fresnel zone pattern," Appl. Opt. **6**(9), 1567–1570 (1967).
12. A. Kołodziejczyk and Z. Jaroszewicz, "Diffractive elements of variable optical power and high diffraction efficiency," Appl. Opt. **32**(23), 4317–4322 (1993).
13. J. M. Burch and D. C. Williams, "Varifocal moiré zone plates for straightness measurement," Appl. Opt. **16**(9), 2445–2450 (1977).
14. N. López-Gil, H. C. Howland, B. Howland, N. Charman, and R. Applegate, "Generation of third order spherical and coma aberrations by use of radially symmetrical fourth order lenses," J. Opt. Soc. Am. A **15**(9), 2563–2571 (1998).
15. I. A. Palusinski, J. M. Sasián, and J. E. Greivenkamp, "Lateral-shift variable aberration generators," Appl. Opt. **38**(1), 86–90 (1999).
16. T. Hellmuth, A. Bich, R. Börret, A. Holschbach, and A. Kelm, "Variable phaseplates for focus invariant optical systems," Proc. SPIE **5962**, 596215 (2005).
17. A. Guirao, D. R. Williams, and I. G. Cox, "Effect of rotation and translation on the expected benefits of an ideal method to correct the eye's higher order aberrations," J. Opt. Soc. Am. A **18**(5), 1003–1015 (2001).
18. E. Acosta and S. Bará, "Variable aberration generators using rotated Zernike plates," J. Opt. Soc. Am. A **22**(9), 1993–1996 (2005).
19. B. M. Pixton and J. E. Greivenkamp, "Spherical aberration gauge for human vision," Appl. Opt. **49**(30), 5906–5913 (2010).

#146873 - $15.00 USD Received 3 May 2011; revised 3 Jun 2011; accepted 10 Jun 2011; published 22 Jun 2011

1. Introduction

Many optical devices and instruments can suffer from aberrations that cause blur and low contrast in captured images, as well as difficulties in sharp focusing. In certain applications only primary spherical aberration dominates. It is well known that focusing through a refractive index mismatch introduces spherical aberration that depends in the focusing depth. Thus, applications such as microscopy [1], optical trapping [2], and optical pick-up [3] among others, need to compensate for spherical aberration for good performance. The difficulties in focussing caused by spherical aberration have been recently exploited as a mechanism for achieving extended depth of field imaging in a hybrid optical-digital system in a technique called spherical coding [4]. These types of applications require a dynamic process to modify the spherical aberration of the system due to the change of the constraints of the system itself. Thus, in some applications, deformable mirrors [5], deformable membranes [1] or liquid crystal lenses [3] have been used as active correcting elements.

An early and interesting optical aberration generator has been proposed by Buchroeder et al. [6]. This generator consists of a set of eleven lenses (plane parallel, cylindrical and spherical doublets) and by means of element tilts, rotations, axial and transversal displacements, a linear combination of aberrations can be generated. A different method for generating variable amounts of a given aberration is the use of phase plates that are displaced or rotated. The well-known method to produce only second order aberrations (defocus and astigmatism) is the Alvarez-Humphrey lens and Lohmann lens [6–9]. It is also possible to generate aberration by means of diffractive elements [10–13].

A method to produce variable amounts of spherical aberration coupled with coma, astigmatism and wavefront tilt has been discussed by López-Gil et al. [14]. A generalization to other aberrations has been proposed by Palusinski et al [15]. Hellmuth et al. [16] proposed and manufactured an adaptive phase plate where third-order aberrations can be adjusted by diagonally displacing two identical but opposite in sign phase plates. All of these approaches are based on the fact that for any aberration characterized by a polynomial expansion of degree n, a lateral displacement Δ of the reference frame gives rise to the appearance of all aberration terms of orders p equal to or smaller than n, whose coefficients are proportional to the powers Δ^{n-p} of the lateral displacement, as can be straightforwardly deduced [17].

Thus, by superimposing two such optical elements, phase plates with complementary signs, the original aberration mode of order n cancels out, and some amounts of lower order terms are produced. The above mentioned phase plates (except the Alvarez-Humphrey and Lohmann lens) generate some amounts of undesired lower order aberrations. This drawback was first overcome for non symmetric aberrations with rotating pairs of phase plates [18]. However, the rotating solution for spherical aberration generates phase dislocations and angular sectors with undesired phases.

The problem of generating spherical aberration using phase plates and without introducing significant unwanted aberrations is of current interest given the variety of systems [1–5,19] that would benefit from its solution. In this paper we discuss a solution to this problem. We use two sets of phase plates that are displaced in perpendicular directions. The result is the ability to generate primary spherical aberration (r^4) or Zernike spherical aberration $(6r^4 - 6r^2 + 1)$ that is proportional to the plate-pair displacement. The simulation results performed in Zemax, optical design software, show ample tolerances to errors in the plate spacing and displacements, and insignificant aberration residual due to other modes.

2. Theory

In this section we describe the physical shape of two phase plate-pairs able to produce a variable amount of a linear combination of quartic and quadratic phase terms. A schematic drawing is shown in Fig. 1.

#146873 - $15.00 USD Received 3 May 2011; revised 3 Jun 2011; accepted 10 Jun 2011; published 22 Jun 2011

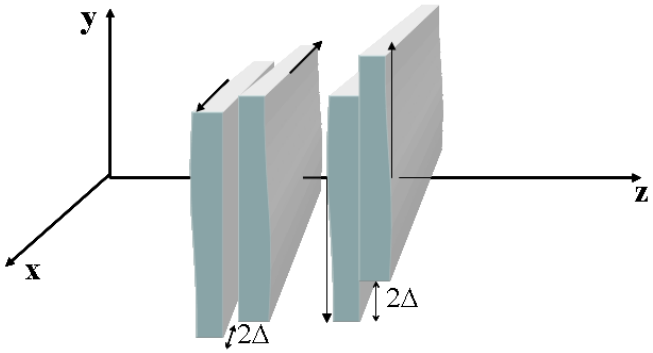

Fig. 1. System of phase plates and way of displacement.

The phase plate system consists of two pairs of phase plates. For the first pair and for the first plate, the first surface is described by,

$$S1(x,y) = A[x^3y^2 + 2xy^4 - \frac{3a}{2}xy^2], \tag{1}$$

where A represents the strength of the plate and *a* can take any real value. The second surface of the first phase plate is flat.

The first face of the second plate is flat and the second surface is also described by Eq. (1) replacing *A* by *–A*. If we assuming parallel light illumination, then when both plates are in contact and displaced by an amount *Δ* in opposite directions along the X coordinate, the resulting optical path difference is proportional to the equivalent thickness of the set in the overlapping region, this is,

$$OPD_1 = A(n-n')[6\Delta x^2y^2 + 2\Delta^3y^2 + 4\Delta y^4 - 3a\Delta y^2], \tag{2}$$

where *n* represents the refractive index of the plate and *n'* that of the surrounding medium. In Eq. (2) some constant phase terms have been neglected and a simple optical path addition has been used to obtain the final optical path difference.

The second phase pair-plate, has also complementary plates with physical shape given by,

$$S2(x,y) = A[\frac{-1}{10}y^5 + \frac{3}{2}yx^4 - \frac{3a}{2}yx^2]. \tag{3}$$

When these plates are in contact and displaced in opposite directions in the Y coordinate by the same amount *Δ*, the optical path difference becomes,

$$OPD_2 = A(n-n')[-\Delta y^4 - 2y^2\Delta^3 + 3\Delta x^4 - 3a\Delta x^2]. \tag{4}$$

Thus, when both pairs of plates are stacked together a linear combination of spherical aberration and defocus proportional to the relative displacement *Δ* is obtained,

$$OPD = 3A(n-n')\Delta[r^4 - ar^2], \tag{5}$$

where $r^2 = x^2 + y^2$. If the parameter *a = 0* only primary spherical aberration is obtained whereas with *a = 1* some defocus is introduced which minimizes the OPD variance (being in fact proportional to Zernike polynomial $(6r^4 - 6r^2 + 1)$. Thus the quadratic terms can be optionally introduced in order to have certain control on the best focus positions. Figure 2 shows in false-colour scale the shapes of the aspherical surfaces for both primary and Zernike spherical aberration.

#146873 - $15.00 USD Received 3 May 2011; revised 3 Jun 2011; accepted 10 Jun 2011; published 22 Jun 2011

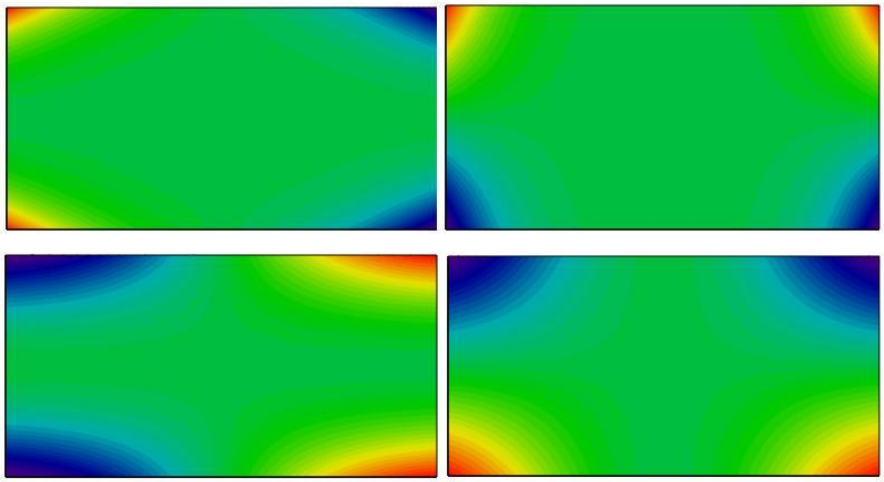

Fig. 2. Surface shapes for classic spherical aberration (top) and Zernike spherical aberration (bottom).

In summary, we point out that the generation of spherical aberration using only one pair of phase plates is accompanied with lower order aberrations such as tilt, coma, and astigmatism [14,15,19]. Our phase plates do not generate such terms at the expense of using two pairs of phase plates that move in orthogonal directions. Both the shape of the plates and the orthogonal character contribute to generate the r^4 and r^2 terms while cancelling lower order terms.

3. Numerical simulations

In developing Eq. (5) we have assumed that the ray intersection coordinates along the four plates are the same and that the system is perfectly aligned with all plates in contact. In practice none of these assumptions are valid. In this section we analyze some tolerances of the plate system by modelling different situations of spacing between plates and misalignments. Without loss of generality we will only show the results for the generation of Zernike spherical aberration.

Our phase plates described by Eqs. (1) and (3) with $a = 1$ were modelled in Zemax optical design software. We used BK7 glass for plates in air and a wavelength of 0.6563μm. Each plate is a square of about 50 mm in side and a thickness of $5\ mm$. The strength parameter A is set to 0.02 to obtain up to ± 8 waves of Zernike spherical aberration for a maximum displacement Δ of $\pm 10 mm$ and a pupil of $25\ mm$ in diameter (about ± 48 waves peak to valley). The resulting wavefront is fitted to 25 Zernike polynomials listed in Table 1.

Table 1. List of Zernike Polynomials Used for the Fit

1	$(10r^5-12r^3+3r)\cos(\theta)$
$r\cos(\theta)$	$(10r^5-12r^3+3r)\sin(\theta)$
$r\sin(\theta)$	$(20r^6-30r^4+12r^2-1)$
$(2r^3-1)$	$r^4\cos(4\theta)$
$r^2\cos(2\theta)$	$r^4\sin(4\theta)$
$r^2\sin(2\theta)$	$(5r^5-4r^3)\cos(3\theta)$
$(3r^3-r)\cos(\theta)$	$(5r^5-4r^3)\sin(3\theta)$
$(3r^3-r)\sin(\theta)$	$(15r^6-6r^4+20r^2)\cos(2\theta)$
$(6r^4-6r^2+1)$	$(15r^6-6r^4+20r^2)\sin(2\theta)$
$r^3\cos(3\theta)$	$(35r^7-60r^5+30r^3-4r)\cos(\theta)$
$r^3\sin(3\theta)$	$(35r^7-60r^5+30r^3-4r)\sin(\theta)$
$(4r^4-3r^2)\cos(2\theta)$	$(70r^8-140r^6+90r^4-20r^2+1)$
$(4r^4-3r^2)\sin(2\theta)$	

#146873 - $15.00 USD Received 3 May 2011; revised 3 Jun 2011; accepted 10 Jun 2011; published 22 Jun 2011

First we assume the plates are aligned but there is some spacing between them due to the optical mounts. Thus a spacing of 3 *mm* between pairs and a spacing of 1 *mm* between plates of each pair is considered for the simulations as shown in Fig. 3.

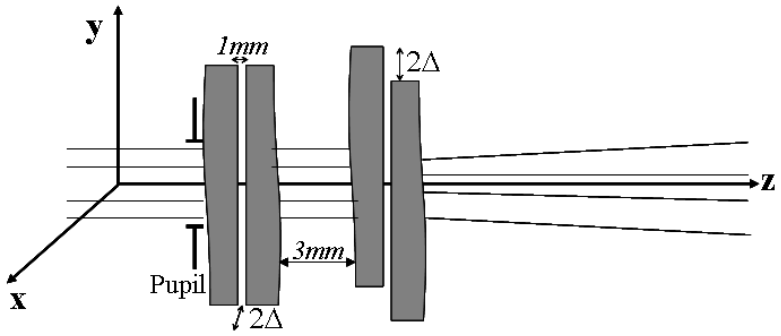

Fig. 3. Phase plate schematic drawing.

The expected linear behaviour of the fit coefficient for the Zernike spherical aberration with the displacement does not appreciably change as shown in Fig. 4.

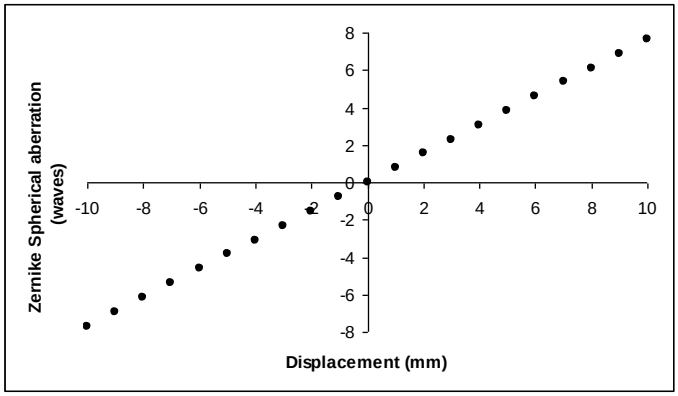

Fig. 4. Variation of the Zernike spherical aberration versus plates displacement.

After subtraction of an optimized value of spherical aberration simulated with an even asphere of 4th degree in the input of the system, the residual aberration peak to valley value of the phase as well as rms value of the phase are plotted in Figs. 5 and 6 respectively. Figure 7 shows some phase maps of the residual aberrations for different values of the displacements. It can be observed that the rms residual error depends on the square of the displacement and less than 0.02 waves rms error is obtained for the maximum displacement of $\Delta = 10mm$ (where about 48 waves of spherical aberration can be achieved).

#146873 - $15.00 USD Received 3 May 2011; revised 3 Jun 2011; accepted 10 Jun 2011; published 22 Jun 2011

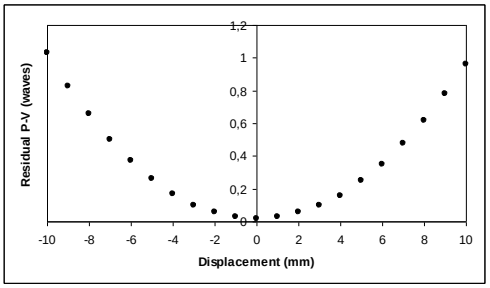

Fig. 5. P-V value of the residual aberration.

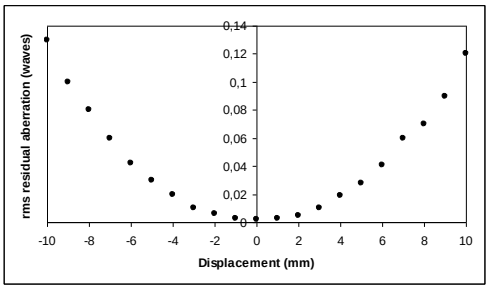

Fig. 6. rms value of the residual aberration.

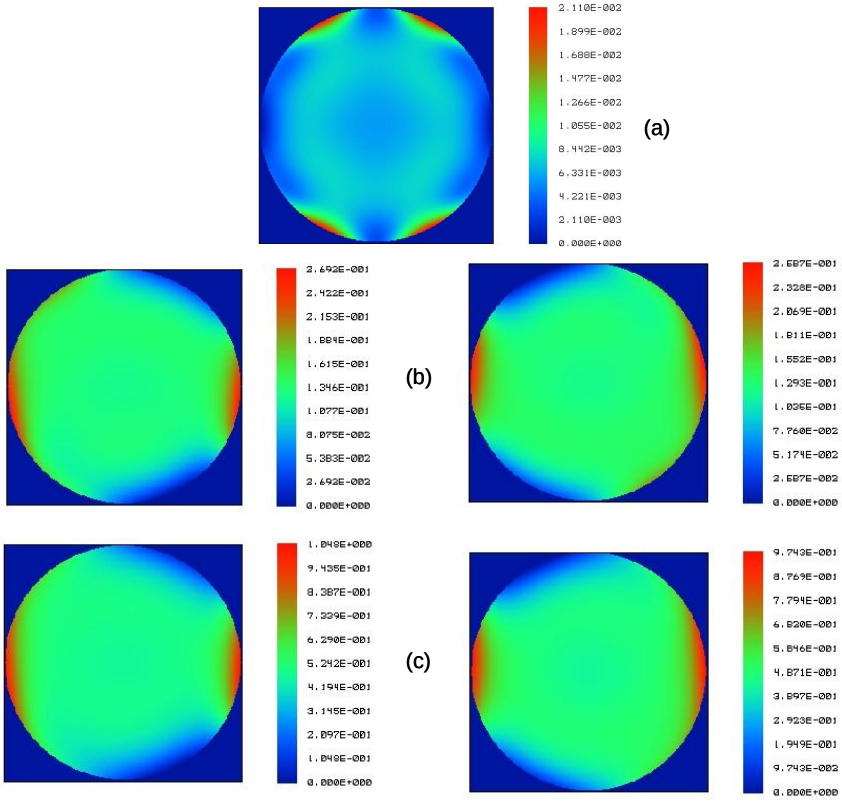

Fig. 7. Phase maps for the residual aberration for displacements between plates of (a) 0mm, (b) + 5mm and –5mm (c) + 10mm and –10mm.

#146873 - $15.00 USD Received 3 May 2011; revised 3 Jun 2011; accepted 10 Jun 2011; published 22 Jun 2011

For analysing the effects of misalignments we show phase maps using the phase plates in the same situation as in (i) but also considering misalignments and rotations of the plates in the following cases: 1) $\Delta = 0mm$ for the first pair and $\Delta = 0.01mm$ for the second pair, 2) $\Delta = 5mm$ for the first pair and $\Delta = 5.01mm$ for the second one, and 3) $\Delta = 10mm$ for the first pair and $\Delta = 10.01mm$ for the second one. In addition, in these three cases the following random values for plate rotations about the axes X,Y, and Z were included in the simulation:

a) The first plate was rotated 0.1 degrees about X, −0.05 about Y and 0.3 about Z

b) The second plate was rotated −0.2 degrees about X, 0.04 about Y and 0.1 about Z

c) The third plate was rotated 0.05 degrees about X, −1.1 about Y and 0.2 about Z

d) The fourth plate was rotated 0.8 degrees about X, 0.05 about Y and 0.1 about Z

The phase maps with spherical aberration removed are shown in Fig. 8. It can be seen that the residual P-V value in the phase error in all cases is not larger than two times the P-V value in the alignment case what also implies a large tolerance to misalignments given the perturbation values chosen.

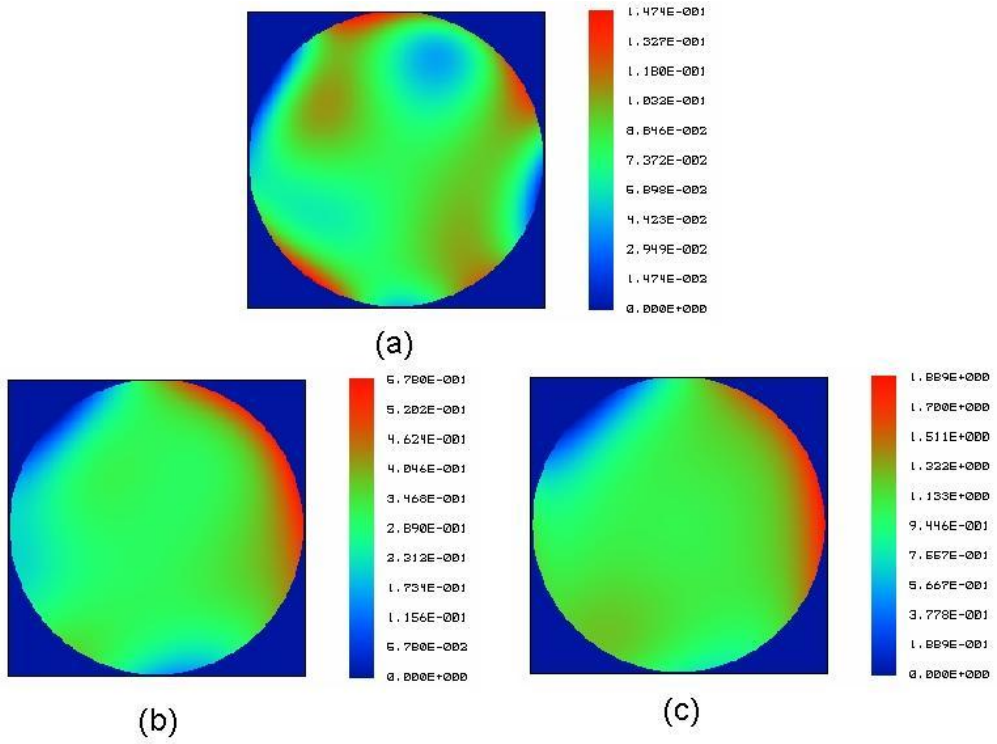

Fig. 8. Phase map (in waves) for a set-up randomly misaligned for displacements of (a) 0mm, (b) 5mm and (c) 10 mm.

The phase plates optical figure error depends on the quality of the final phase error specified. Thus for a $\lambda/4$ maximum phase transmitted error and using the RSS (Root of Sum Squares) error rule, the individual eight surfaces must be approximately made to $\lambda/4\sqrt{8}\,(n-1)$.

4. Conclusion

We have presented a set of phase plate-pairs for the generation of a variable amount of primary spherical aberration. This amount is proportional to the relative lateral displacement

#146873 - $15.00 USD Received 3 May 2011; revised 3 Jun 2011; accepted 10 Jun 2011; published 22 Jun 2011

of each pair. It is noteworthy that the numerical simulations under realistic (and quite extreme) experimental constraints show that the system is tolerant to both the spacing between plates, as well as to misalignments and rotations of each of the plate components.

Our phase-plate design is different in its inner working principle. Rather than using a differential movement in one direction as in earlier phase plates, it uses a superposition of two differential movements in orthogonal directions to generate spherical aberration. In this way, no lower modes are generated and the residual higher modes are not significant. Although the implementation of four plates could seem a disadvantage, the system is tolerant to misalignments even for large displacements that are required to generate a large amount of spherical aberration. Considering that the problem of the generation of a variable amount of spherical aberration is still of importance in many fields, the use of four plates is nevertheless an attractive solution. This solution is an inexpensive and robust alternative to other means, not necessarily less complex or easily implemented such as deformable mirrors. Furthermore, both primary spherical aberration and Zernike spherical aberration can be generated with our proposed phase plates.

Acknowledgments

This work was supported by the Spanish Ministerio de Educacion y Ciencia grant FIS2010-16753 and the FEDER and performed during the sabbatical stay of E. Acosta at the University of Arizona.

#146873 - $15.00 USD Received 3 May 2011; revised 3 Jun 2011; accepted 10 Jun 2011; published 22 Jun 2011